Earth, Moon, and Planets (2005) 94: 31–40
DOI 10.1007/s11038-004-6816-5

CHALLENGES FROM SOLID EARTH DYNAMICS FOR SATELLITE GRAVITY FIELD MISSIONS IN THE POST-GOCE ERA

BERT L. A. VERMEERSEN
DEOS, Delft University of Technology, Kluyverweg 1, 2629 HS, Delft, The Netherlands
(E-mail: b.vermeersen@lr.tudelft.nl)

(Received 11 August 2004; Accepted 25 November 2004)

Abstract. Examples from four main categories of solid-earth deformation processes are discussed for which the GOCE and GRACE satellite gravity missions will not provide a high enough spatial or temporal resolution or a sufficient accuracy. Quasi-static and episodic solid-earth deformation would benefit from a new satellite gravity mission that would provide a higher combined spatial and temporal resolution. Seismic and core periodic motions would benefit from a new satellite mission that would be able to detect gravity variations with a higher temporal resolution combined with very high accuracies.

Keywords: Deformation, gravity, resolution

1. Introduction

In solid-earth research after the GOCE mission the interest in temporal variations of the gravity field will be increasing. As far as effects near the Earth's surface are concerned, many requirements will not be met by the spatial resolution of temporal variations observed by GRACE.

Three main areas of solid-earth geodynamics can be distinguished on which solid-earth dynamics would benefit from a "GRACE-like", or even better, temporal resolution for "GOCE-like" spatial scales: post-glacial rebound and concomitant sea-level variations; co- and post-seismic solid-earth deformation; and mantle convection and plate tectonics.

The situation is different for the detection of core motions and seismic modes, where the spatial resolution is not critical for core motions, but a very high accuracy and temporal resolution are required.

In the following sections, each of these four geodynamical processes and their geodetic signatures are briefly introduced, after which an overview is given of what GRACE and GOCE are expected to contribute to each of these fields, and where GRACE and GOCE fall short.

It should be noted that gravity effects from crustal displacements due to hydrological, oceanic and atmospheric loadings are not treated here.

2. Glacial Rebound and Associated Sea Level Variations

Glacial Isostatic Adjustment (GIA) of the solid Earth due to the waxing and waning of Late-Pleistocene Ice-Age cycles has created geoid and gravity anomalies, although the separation between GIA-induced contributions and those induced by plate tectonics and mantle dynamics is not always obvious. For example, it is now widely acknowledged that the deep geoid low above Canada is partly due to non-GIA induced lithosphere and mantle heterogeneities and partly attributable to GIA (e.g., Simons and Hager, 1997).

Whereas the geoid above Canada is related to (at least) two geodynamical processes, it is thought that secular geoid and gravity anomaly variations are only triggered by post-glacial rebound (e.g., Wahr and Davis, 2002). Figure 1, taken from Wahr and Davis (2002), shows in the top panel the secular degree geoid amplitude as function of spherical harmonic degree for expected GRACE errors and predictions of three models: GIA; present-day Antarctic ice decay equivalent with a sea-level

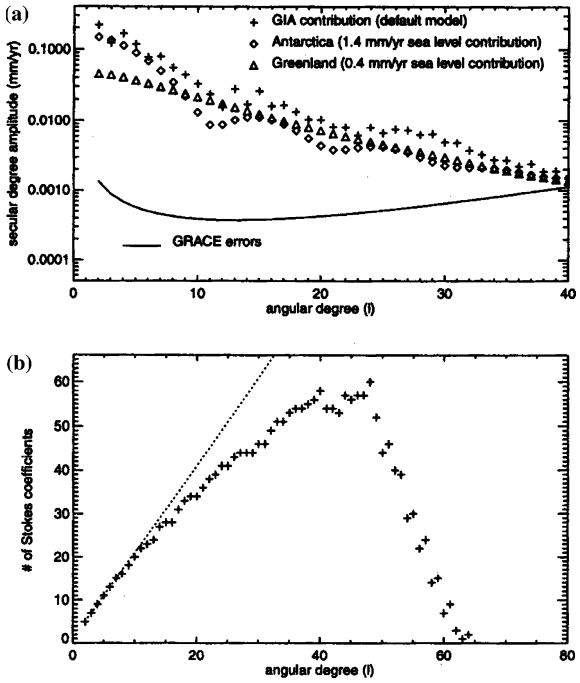

Figure 1. (a) Present-day secular geoid change model predictions for GIA due to Late-Pleistocene deglaciation with a default model (see text for details), together with the effects of the maximum contemporary melt scenarios for the Antarctic and Greenland ice caps. The solid line represents the predicted errors in the GRACE data; (b) Total number of Stokes coefficients as function of spherical harmonic degree for which the GIA signal of *a* is expected to be larger than the expected secular GRACE measurement error (*figure taken from Wahr and Davis, 2002*).

rise of 1.4 mm/yr; and present-day Greenland ice cap decay equivalent with a sea-level rise of 0.4 mm/yr.

The default model for the GIA contribution has an earth model with a lithospheric thickness of 120 km and upper and lower mantle viscosities of 10^{21} and 10^{22} Pa s, respectively, while the radial elastic and constitutional parametrization is based on the Preliminary Reference Earth Model (PREM) by Dziewonski and Anderson (1981) and the Late-Pleistocene ice-decay model is based on ICE-3G by Tushingham and Peltier (1991). From this top panel of Figure 1 it can be derived that GRACE is expected to be able to discern GIA and (maximum) present-day Antarctic and Greenland ice-cap variations up to about harmonic degree 40. For degrees between about 40 and 60, still a number of Stokes coefficients related to the defaults GIA model are expected to become detectable by GRACE, as is shown in the lower panel of Figure 1. In total, for all harmonic degree up till degree 60 about 2000 Stokes coefficients should become detectable. It should be noted here that the pre-launch estimates of GRACE as given in Figure 1 are considerably higher than what is achieved in the most recent models. For instance, compare with Figure 1 of Tapley et al. (2004), taking into account that the GRACE uncertainty estimates in Figure 1 are based on a 5-year mission length.

Figure 2, also taken from Wahr and Davis (2002), shows the sensitivity of mantle viscosity and lithospheric thickness variations in GIA models with respect to secular GRACE measurement errors. The data points represent differences between two lower mantle viscosity models "v_{LM}", two upper mantle viscosity models "v_{UM}" (viscosities given in Pa·s) and two lithospheric thickness models "lith".

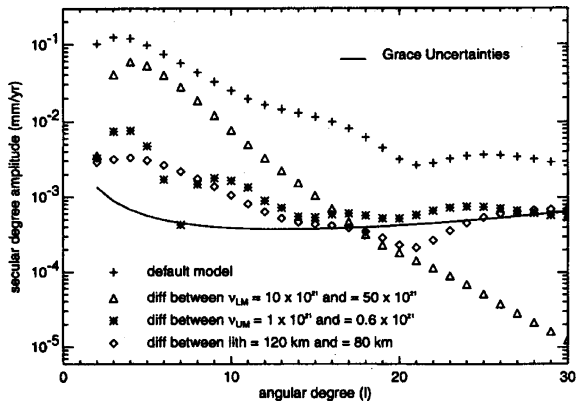

Figure 2. Comparison of the difference in degree amplitudes between three GIA models having varying viscosities and lithosphere thickness and the default GIA model, with respect to expected GRACE measurement errors (*figure taken from Wahr and Davis, 2002*).

From Figure 2 it is clear that differences in mantle viscosity and lithospheric thickness are expected to become discernible from GRACE data till about degree 15, whereby lower mantle viscosity shows the highest sensitivity. However, this figure does not show what the influence on these sensitivities is from uncertainties in present-day ice-sheet variations and from uncertainties in the Late-Pleistocene ice models.

To summarize, Figures 1 and 2 show that in the most optimistic scenarios, i.e. in the (presently about a factor of 40 too optimistic) prelaunch estimates as depicted in both figures, GRACE might be able to detect GIA motions and present-day Antarctic and Greenland ice mass decay up to harmonic degree 40, and might be able to distinguish mantle viscosity and lithosphere thickness in solid-earth models up to harmonic degree 15. This might be sufficient for discriminating between the effects of GIA above Canada and present-day Greenland ice cap changes, something which cannot be done presently with SLR dJ_n/dt observations (e.g., Vermeersen et al., 2003). Figure 2 shows that if the GRACE error curve could be lowered for harmonic degrees above 15, additional information would become available on especially lithosphere thickness and shallow mantle viscosity.

In various continental regions, seismic observations indicate the presence of shallow low-viscosity zones (intra-crustal layers, asthenosphere). Due to their shallowness, these low-viscosity zones can create high-harmonic patchlike anomalies superimposed on the low-harmonic geoid as the aforementioned broad and deep Canadian one, with typical magnitudes on the cm to m level for spatial scales of 100–1000 km (Vermeersen, 2003).

The high-harmonic geoid signatures resulting from the presence of low-viscosity zones are about one to two orders smaller than the low-harmonic geoid signatures induced by large-scale mantle flow triggered by GIA. Similarly, the temporal changes are about one or two orders of magnitude smaller and are thus not detectable by GRACE. An example of the geoid anomalies for Fennoscandia that is expected to be detectable by GOCE is given in Figure 3 (van der Wal et al., 2004).

3. Co- and Post-seismic Deformation

Large earthquakes induce local, regional and global gravity field variations, both during and in the days, months, years and tens of years after the faulting event. The harmonic components will be treated in section *d*; here the episodic co- and and post-seismic displacements are considered.

During a faulting event there is an immediate, non-recoverable redistribution of the Earth's mass. This is called co-seismic deformation. Due to the existence of shallow low-viscosity intra-crustal and asthenospheric layers, the redistribution of stress and strain due to the faulting will relax in the days,

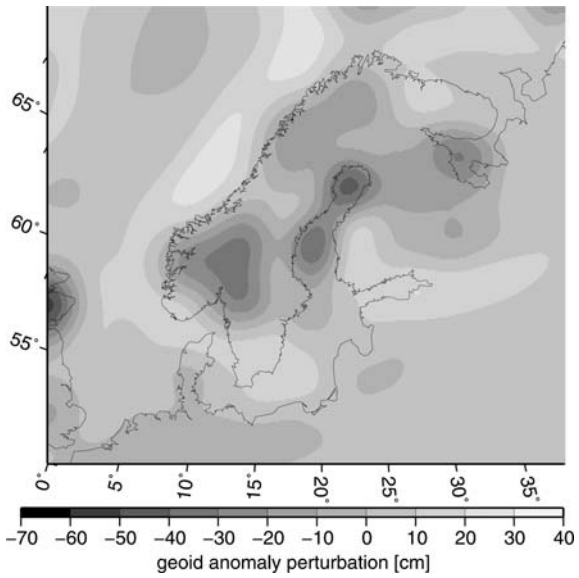

Figure 3. Simulated present-day differential geoid anomalies for the northern part of Europe due to a crustal low-viscosity zone at 20 km depth with a thickness of 12 km and a viscosity of 10^{18} Pa s, as a consequence of solid-earth deformation resulting from Late-Pleistocene Ice-Age cycles. The figure shows the geoid anomaly differences between the earth model with the aforementioned low-viscosity crustal zone and without such a low-viscosity zone in the 80 km thick lithosphere.

months, years and tens of years after the earthquake. This relaxation is not necessarily diminishing the co-seismic mass redistribution; the post-seismic deformation can enhance this.

Co- and post-seismic deformation due to large earthquakes might be detectable from space, depending on the parameters of the earthquake source, such as seismic moment (being the product of the solid-earth rigidity at the fault, fault length and relative fault displacement), type of earthquake (e.g., normal fault, strike-slip fault), geometry of the faulting event and depth of the earthquake (e.g., Sabadini and Vermeersen, 1997).

For example, Figure 4, taken from Gross and Chao (2002), shows the co-seismic effects of the great Chile earthquake of May 1960 (seismic moment of 5.5×10^{23} Nm) and the great Alaska earthquake of March 1964 (seismic moment of 7.5×10^{22} Nm), together with two largest ones during the period 1965–2000: the Sumba earthquake of August 1977, having a seismic moment of 3.6×10^{21} Nm; and the Macquarie one of May 1989, having a seismic moment of 1.4×10^{21} Nm.

Figure 4 indicates that GRACE, if it would have been active in the time frame from early 1960 to the end of 1964, should have been able to detect the co-seismic gravitational field changes of the Chile and Alaska earthquakes up to about harmonic degree 60 for the Alaskan event and up to about degree 80

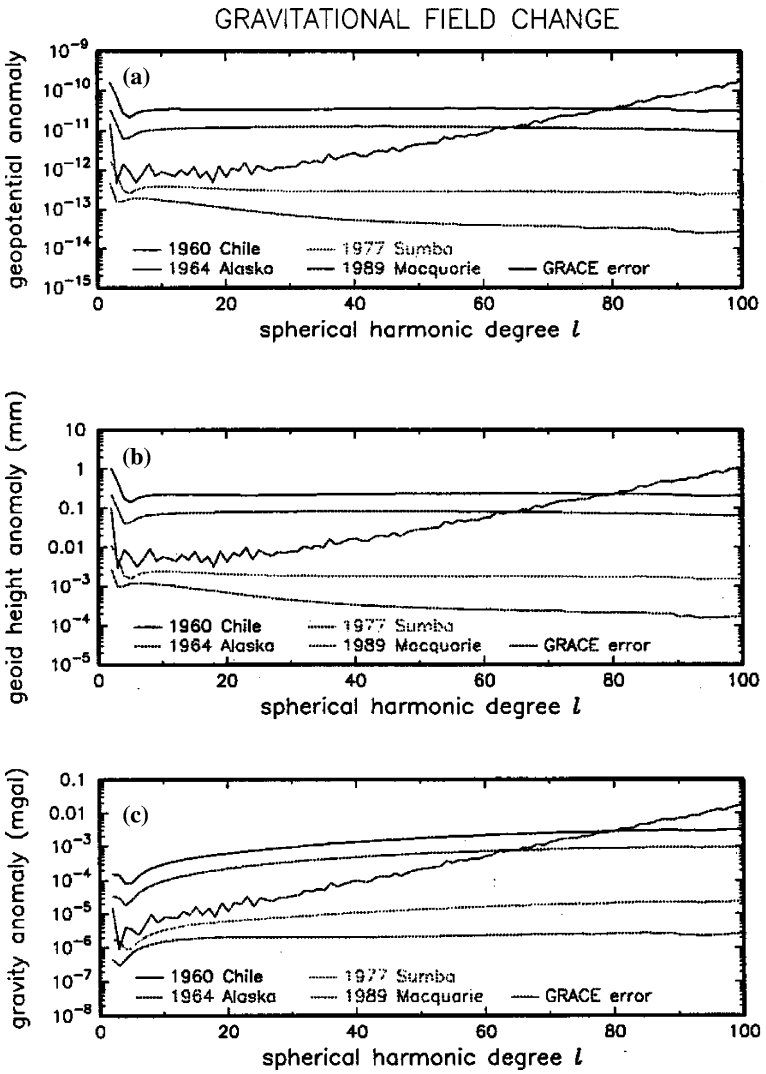

Figure 4. Gravity and geoid effects of co-seismic deformation due to four selected earthquakes, together with the expected instrumental errors of the GRACE measurements (*figure taken from Gross and Chao, 2002*).

for the Chilean event. The co-seismically induced gravitational field changes from the other two earthquakes fall below the detection level of GRACE, implying that no co-seismic effects of earthquakes would have been detected if GRACE would have been operative in the 1965–2000. Post-seismic deformation due to viscous flow of shallow low-viscosity layers in the Earth could significantly enhance or reduce the signals, and also hydrological changes associated with the stress and strain redistribution close to the fault can significantly impact crustal displacements and gravity signals.

A related issue to co-seismic deformation are ionospheric perturbations. Doppler ionospheric soundings indicate that after strong earthquakes the ionized layers E and F show displacement of several tens of meters (e.g., Artru et al., 2001). It is unclear at the moment what the gravity perturbations associated with these ionospheric layer displacements are. It might be that they are negligible in magnitude compared to the direct gravity changes from the solid Earth, but, on the other hand, the induced ionospheric perturbations are closer to the satellites than the direct solid-earth displacements.

4. Mantle Convection and Plate Tectonics

Mantle convection and one of its most prominent features, subduction of oceanic plates, show up in the geoid most conspicuously at low spherical harmonics (degrees 4–9), although also at higher degrees there are contributions (e.g., King, 2002). Apart from these quasi-static signals, it is expected that there are a number of geologically ''fast'' temporal changes associated with the mantle convection cylce and plate tectonics. Examples include fast rising upper-mantle plumes (e.g., Larsen, 1997), sinking slabs (e.g., Piromallo et al., 1997) and fast sinking detached slabs (e.g., Schott and Schmeling, 1998). Numerical models show that these phenomena can produce temporal geoid variation signals up to 0.1–1 mm/yr.

But higher rates are possible as well for more localized processes, e.g., for fast subsidence or emergence of oceanic islands and fast movements in volcanic regions. With the latter, also the shedding of volcanic ashes into the atmosphere during an eruptive phase might contribute to detectable temporal gravity variations.

5. Core Motions and Seismic Modes

Figure 5, taken from Crossley et al. (1999) (see also Hinderer and Crossley, 2000), gives an overview of typical normalized amplitudes of surface gravity variations due to core motions and seismic events, and the time scales on which they occur or are predicted to occur.

The ''Slichter Triplet'' in Figure 5 refers to a gravito-inertial translation of the solid inner core, while ''FCN'' and ''FICN'' stand for Free (Inner) Core Nutation. FCN occurs whenever there is an angle between the rotation axes of the liquid outer core and the mantle, with its eigenfrequency being proportional to the flattening of the outer core. The same with FICN, but then with respect to the solid inner core.

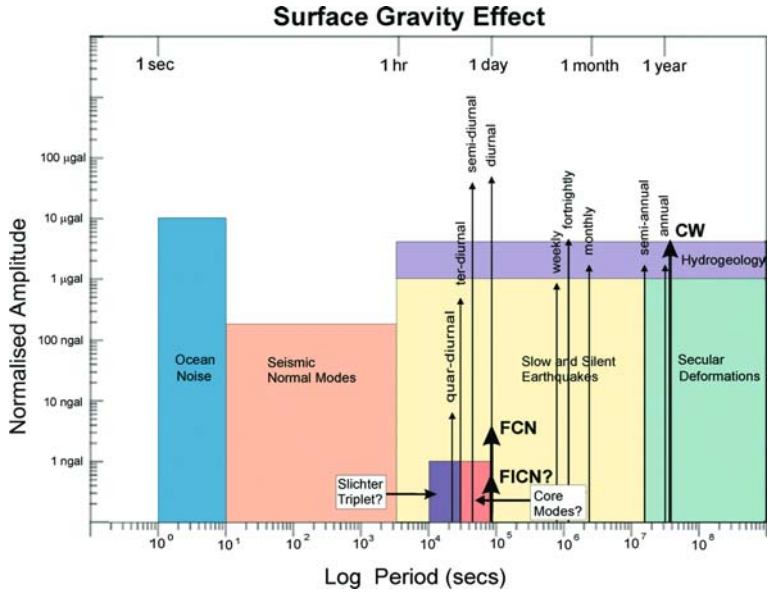

Figure 5. Typical gravimetic effects of core motions and seismic events, using harmonic amplitude harmonization (*figure taken from Crossley et al.,* 1999).

Observing the FICN would enhance our hitherto scarce knowledge of the flattening of the inner core boundary and the density jump at the inner-outer core interface.

The effects of quasi-static displacements during and after an earthquake have already been considered in the section on co- and post-seismic deformation; in Figure 5 the harmonic components of seismic faulting events are treated (*seismic normal modes*), and earthquakes that do not show up in seismograms but do show up in free oscillation observations (*slow earthquakes*) and earthquakes that do not show up in seismograms nor in free oscillation measurements (*silent earthquakes*).

Apart from the Chandler Wobble (''CW'' in Figure 5), there are decadal fluctuations in the Earth's gravity field due to wobbling of the inner core. These might just reach the detection level of GRACE: Greiner-Mai et al. (2000) finds that the predicted rates of change of the Stokes coefficients C_{2m} and S_{2m} by this process averaged over a time frame of 10 years are: $C_{21} = -6.0 \times 10^{-12}$ yr^{-1}; $S_{21} = 1.0 \times 10^{-11}$ yr^{-1}; $C_{22} = -1.6 \times 10^{-12}$ yr^{-1}; and $S_{22} = -1.8 \times 10^{-12}$ yr^{-1}. The estimated standard deviations of the low-degree (<5) coefficients for GRACE are 2×10^{-12} yr^{-1} for 1 year of data, and 10^{-13} for 5 year of data. However, this decadal signal might ''drown'' in the contributions that other geophysical processes induce in C_{2m} and S_{2m} temporal variations.

Acknowledgements

This study was funded by Astrium under an Enabling Technology study contract. Two anonymous reviewers are thanked for their constructive comments on an earlier draft of this paper.

References

Artru, J., Lognonne, Ph., and Blanc, E.: 2001, 'Normal Modes Modelling of Post-Seismic Ionospheric Oscillations', *Geophys. Res. Lett.* **28**(4), 697–700.

Crossley, D., Hinderer, J., Casula, G., Francis, O., Shu, H.-T., Imanishi, Y., Jentzsch, G., Kaarianen, J., Merriam, J., Meurers, B., Neumeyer, J., Richter, B., Shibuya, K., Sato, T., and van Dam, T.: 1999, 'Network of Superconducting Gravimeters Benefits a Number of Disciplines', *EOS Trans. Am. Geophys. U.* **80**, 121–126.

Dziewonski, A. M. and Anderson, D. L.: 1981, 'Preliminary Reference Earth Model (PREM), *Phys. Earth Planet. Inter.* **25**, 297–356.

Greiner-Mai, H., Jochmann, H., and Barthelmes, F.: 2000, 'Influence of Possible Inner-Core Motions on the Polar Motion and the Gravity Field', *Phys. Earth Planet. Inter.* **117**, 81–93.

Hinderer, J. and Crossley, D.: 2000, 'Time Variations in Gravity and Inferences on the Earth's Structure and Dynamics', *Surv. Geophys.* **21**(1), 1–45.

Gross, R. S. and Chao, B. F.: 2002, 'The Gravitational Signature of Earthquakes', in M. G. Sideris (ed.), *Gravity, Geoid and Geodynamics 2000*, Springer, IAG Geodesy Symposia, **123**, pp. 205–210.

King, S.: 2002, 'Geoid and Topography Over Subduction Zones: The Effect of Phase Transformations', *J. Geophys. Res.* **107**(B1), doi:10.1029/2000JB000141.

Larsen, T. B. and Yuen, D. A.: 1997, 'Ultrafast Upwelling Bursting Through the Upper Mantle', *Earth Planet. Sci. Lett.* **146**, 393–400.

Piromallo, C., Spada, G., Sabadini, R., and Ricard, Y.: 1997, 'Sea-level Fluctuations Due to Subduction: The Role of Mantle Rheology', *Geophys. Res. Lett.* **24**, 1587–1590.

Sabadini, R. and Vermeersen, L. L. A.: 1997, 'Influence of Lithospheric and Mantle Layering on Global Post-Seismic Deformation', *Geophys. Res. Lett.* **24**, 2075–2078.

Schott, B. and Schmeling, H.: 1998, 'Delamination and Detachment of a Lithospheric Root', *Tectonophys.* **296**(3–4), 225–247.

Simons, M. and Hager, B. H.: 1997, 'Localization of the Gravity Field and the Signature of Glacial Rebound', *Nature* **390**, 500–504.

Tapley, B. D., Bettadpur, S., Watkins, M., and Reigber, C.: 2004, 'The Gravity Recovery and Climate Experiment: Mission Overview and Early Results', *Geophys. Res. Lett.* **31**, L09607, doi:10.1029/2004GL019920.

Tushingham, A. M. and Peltier, W. R.: 1991, 'ICE-3G: A New Global Model of Late Pleistocene Deglaciation Based Upon Geophysical Predications of Postglacial Relative Sea Level Change', *J. Geophys. Res.* **96**, 4497–4523.

van der Wal, W., Schotman, H. H. A., and Vermeersen, L. L. A.: 2004, 'Geoid Heights Due to a Crustal Low Viscosity Zone in Glacial Isostatic Adjustment Modeling: a Sensitivity Analysis for GOCE', *Geophys. Res. Lett.* **31**, L05608, doi: 10.1029/2003GL019139.

Vermeersen, L. L. A.: 2003, 'The Potential of GOCE in Constraining the Structure of the Crust and Lithosphere From Post-Glacial Rebound', *Space Sci. Rev.* **108**(1–2), 105–113.

Vermeersen, L. L. A., Schott, B., and Sabadini, R.: 2003, 'Geophysical Impact of Field Variations', in Ch. Reigber, H. Lühr, and P. Schwintzer (eds.), *First CHAMP Mission*

Results for Gravity, Magnetic and Atmospheric Studies, Springer-Verlag, Heidelberg, 165–173.

Wahr, J. M. and Davis, J. L.: 2002, 'Geodetic Constraints on Glacial Isostatic Adjustment', in J. X. Mitrovica, and L. L. A. Vermeersen (eds.), *Ice Sheets, Sea Level and the Dynamic Earth, Geodynamics Series,* American Geophysical Union, Washington, **29**, 3–32.